

Substituent Effects in the Unimolecular Fragmentation of Anisole Dication Derivatives[†]

Jana Roithová, Detlef Schröder,* and Helmut Schwarz

Institut für Chemie der Technischen Universität Berlin, Straße des 17. Juni 135, D-10623 Berlin, Germany

Received: February 2, 2004; In Final Form: April 8, 2004

The unimolecular fragmentation of metastable anisole dications is studied by tandem-mass spectrometry. Permutations of OH, OCH₃, and NH₂ substituents as well as extensive labeling experiments are used as probes to unravel the mechanisms of the various fragmentation pathways observed. The main channel corresponds to methyl ion elimination, which leads to an energetically favorable charge separation (“Coulomb explosion”). Loss of a neutral CO molecule forms another important branch, and the expelled CO has incorporated a carbon atom from the phenyl ring of anisole. Substitution of the anisole dication with OH, OCH₃, and NH₂ groups results in more specific fragmentations. *Ortho*- and *para*-substitutions lead to preferential methyl ion elimination, whereas *meta*-substitution favors CO loss. The substituent effects are also reflected in pronounced changes in the apparent kinetic isotope effects upon substitution of OCH₃ by OCD₃. On the basis of the various experimental findings and some explorative DFT calculations, possible mechanisms for the skeletal rearrangements prior to CO elimination are proposed.

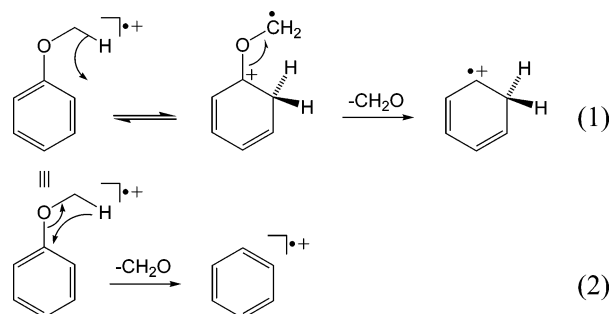
Introduction

Molecular dications challenge the mnemonics of chemical bonding, because of the strongly repulsive electrostatic interactions between the charge-carrying centers. Accordingly, the chemistry of molecular dications often differs very much from that of the corresponding neutral or monocationic counterparts. In fact, a comparison of the charge states 0, +1, and +2 aimed at deriving some common features is not meaningful for most small molecules, because the differences caused by electronic effects are much too drastic.^{1,2} In very large molecules, on the other hand, Coulomb repulsion of the charged centers may only be regarded as a minor perturbation such that, to a good approximation, the chemistry may be viewed as a superposition of the behavior of the corresponding monocationic species.³ Accordingly, borderline cases are expected to occur with medium-sized molecules.

As a probe molecule, we have chosen anisole (methoxybenzene) **1**, which is sufficiently large to form a molecular dication on one hand, while being small enough to show pronounced effects due to Coulomb repulsion. The aim of this work is to investigate how the chemical behavior of anisole is influenced when it is doubly ionized and to what extent substituent effects play a role, when the anisole dications carry substituents in *ortho*-, *meta*-, or *para*-positions. A more fundamental question in this context is whether doubly charged arenes still preserve the common substituent effects of aromatic compounds or if their reactivity is merely controlled by charge-separation (“Coulomb explosion”) processes.^{4,5}

Unimolecular reactions have proven to be an efficient tool for the investigation of ion structures as well as the extensive rearrangements that often follow the ionization of aromatic compounds.^{6–9} The gas-phase chemistry of unimolecular fragmentation of singly charged anisole and substituted anisoles has been the subject of numerous studies.^{10–13} The prevailing channel corresponds to the loss of CH₂O. It has been established¹⁰ that two different reaction mechanisms lead to this

SCHEME 1



product. The first mechanism starts with a five-center rearrangement of a hydrogen atom from the methoxy group to the *ortho*-position of the ring and finally gives rise to an isobenzene cation (reaction 1 in Scheme 1). The initial hydrogen rearrangement is reversible, which has been shown by labeling experiments: if the methyl substituent is labeled by three deuterium atoms (**1b**⁺), losses of CD₂O and CHDO, respectively, appear in the spectra of metastable ions.¹⁴ A similar H/D scrambling is observed also in other fragments, e.g. both CD₃⁺ and CHD₂⁺ eliminations are observed. The second mechanism involves a four-center rearrangement of hydrogen to the *ipso*-position of the ring, which finally leads to the more stable benzene cation (reaction 2 in Scheme 1). For the monocationic species, the branching ratio between reactions 1 and 2 is strongly influenced by the substitution pattern of anisole.¹⁰

Experimental and Computational Details

The experiments were performed with a modified VG ZAB/HF/AMD four-sector mass spectrometer of BEBE configuration (B stands for magnetic and E for electric sector), which has been described in detail previously.¹⁵ The cations and dications of interest were generated by 70 eV electron ionization of the corresponding neutral precursor molecules (Chart 1), accelerated by a potential of 8 kV and mass-selected by means of B(1)/E(1). The unimolecular fragmentations of metastable ions (MI)

[†] Dedicated to Prof. Leo Radom, Sydney, on the occasion of his 60th birthday.

CHART 1

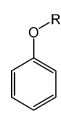
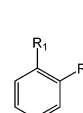
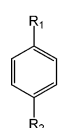
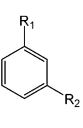
	1	R			4	R ₁	R ₂
1a	CH ₃			4a	OCH ₃	OH	
1b	¹³ CH ₃			5	OCD ₃	OH	
1c	CD ₃			28	OCH ₃	OCD ₃	
						NH ₂	
	2	R ₁	R ₂		6	R ₁	R ₂
2a	OCH ₃	OH		6a	OCH ₃	OH	
3	OCD ₃	OH		6a	O ¹³ CH ₃	OH	
3a	OCH ₃	OCD ₃		6b	OCD ₃	OH	
27	OCH ₃	NH ₂		6c	OCH ₃	OD	
				6d	OCH ₃	¹⁸ OH	
				7	OCH ₃	OCD ₃	
				29	OCH ₃	NH ₂	

TABLE 1: Mass Spectra of Metastable Anisole Dications 1²⁺–1c²⁺ and Relative Kinetic Isotope Effects (KIEs) Obtained As the Ratio of CO-Loss Intensity for the Unlabeled and the Respective Labeled Anisole Dication

	CH ₃ ⁺	¹³ CH ₃ ⁺	CD ₃ ⁺	CHD ₂ ⁺	CO	KIE
1 ²⁺ ^a	100				13.7	1.0
1a ²⁺		100			9.0	1.5
1b ²⁺			100		0.5	27
1c ²⁺ ^a				100	3.0	4.6

^a The species containing one ¹³C were taken as parent ions, and the intensities are accordingly corrected; see experimental details.

occurring in the field-free region preceding the second magnet were monitored by scanning B(2); this will be referred to as MI spectra. Fragment ions arising from fragmentations of metastable parent dications were characterized by their collisional activation spectra (MI/CA). To this end, the parent ions were mass-selected by B(1), and the daughter ion originating from unimolecular fragmentation in the field-free region between B(1) and E(1) was selected by means of E(1) and collided with oxygen (80% transmission) in the field-free region between E(1) and B(2) while the latter sector was scanned to monitor the ionic fragments. All spectra were accumulated with the AMD-Intectra data systems; 5–15 scans were averaged to improve the signal-to-noise ratios. Final data were derived from two to four independent measurements with an experimental error smaller than ±5%. The averaged spectra were normalized to the base peak, which was set to 100. To avoid overlaps in the spectra of dications of even-numbered masses (1²⁺, 1c²⁺, 2²⁺, 4²⁺, 6²⁺) with isobaric monocations, the naturally abundant dications with one ¹³C atom were investigated in the measurements. The intensities given in the Tables 1 and 3, respectively, were accordingly corrected for the one-seventh contribution of the ¹³C isotopologs.

All chemicals were synthesized by standard laboratory procedures. The [¹³CH₃]-labeled compounds (1a and 6a) and the [CD₃]-labeled compounds (1b, 2a, 3, 4a, 5, 6b, and 7) were prepared from the corresponding [OH]-precursors by reaction with ¹³CH₃I (99% ¹³C) and (CD₃)₂SO₄ (99.8 atom % D), respectively. The [¹⁸OH]-labeled compound 6d was obtained from *meta*-anisidin via preparation of the corresponding diazonium salt with [BF₄][−] as a counterion. The salt was dried and then thermally decomposed in the presence of H₂¹⁸O (95 atom % ¹⁸O).

The calculations were performed using the density functional method UB3LYP^{16–18} in conjunction with Dunning's correlation consistent triple- ζ basis set (cc-pVTZ)^{19–21} as implemented in the Gaussian 98 package of programs.²² For all optimized structures, frequency analysis at the same level of theory was used in order to assign them as genuine minima on the PES and in order to calculate zero-point vibrational energy (ZPVE).

TABLE 2: B3LYP/cc-pVTZ Total Electronic Energies (E_e) and Energies at 0 K (E_{0K}) (E_e + ZPVE) of Singlet and Triplet States of Anisole 1²⁺ Dication, Hydroxy-Substituted Anisole Dications 2²⁺, 4²⁺, and 6²⁺, and Some Other Dications and Cations Discussed in the Text, and Relative Energies (E_{rel} in eV) at 0 K with the Anisole Dication 1²⁺ or the *para*-Hydroxyanisole Dication 2²⁺ as Reference Points

ion	state	E_e (hartree)	E_{0K} (hartree)	E_{rel} (0 K) (eV)
1 ²⁺	¹ A'	−346.093 339	−345.962 879	0
	³ A'	−346.075 104	−345.945 938	0.46
8 ⁺ (+CH ₃) ^{a,b}	¹ A	−306.624 233	−306.532 092	−0.90
	³ A''	−306.600 824	−306.510 664	−0.32
10 ²⁺	¹ A	−346.116 155	−345.985 615	−0.62
	³ A	−346.050 888	−345.923 076	1.70
2 ²⁺	¹ A'	−421.402 100	−421.265 177	0
	³ A'	−421.351 206	−421.217 189	1.31
4 ²⁺	¹ A'	−421.385 750	−421.249 322	0.43
	³ A'	−421.364 633	−421.229 267	0.98
6 ²⁺	¹ A'	−421.368 920	−421.233 180	0.87
	³ A'	−421.369 721	−421.234 710	0.83
	¹ A'	−381.912 787	−381.815 121	−0.38
11 ⁺ (+CH ₃) ^{a,b}	¹ A'	−381.912 787	−381.815 121	−0.38
12 ²⁺	¹ A	−421.373 670	−421.239 253	0.71
14 ⁺ (+CH ₃) ^{a,b}	¹ A'	−381.912 877	−381.815 122	−0.38
16 ²⁺	¹ A	−421.394 972	−421.259 315	0.16
17 ⁺ (+CH ₃) ^{a,b}	¹ A'	−381.880 386	−381.784 049	0.47
	³ A''	−381.866 709	−381.772 142	0.79
18 ²⁺	¹ A	−421.404 634	−421.268 079	−0.08
	³ A	−421.322 374	−421.190 209	2.04
19 ²⁺	¹ A	−421.397 407	−421.260 920	0.12
	³ A	−421.340 055	−421.206 620	1.59

^a E_e and E_{0K} are given for cations 8⁺, 10⁺, 14⁺, and 17⁺, whereas E_{rel} (0 K) are given for the sum $E_{0K}(8^+) + E_{0K}(CH_3^+)$, $E_{0K}(10^+) + E_{0K}(CH_3^+)$, $E_{0K}(14^+) + E_{0K}(CH_3^+)$, and $E_{0K}(17^+) + E_{0K}(CH_3^+)$, respectively. ^b $E_e(CH_3^+) = -39.495 186$ hartree, $E_{0K}(CH_3^+) = -39.463 995$ hartree.

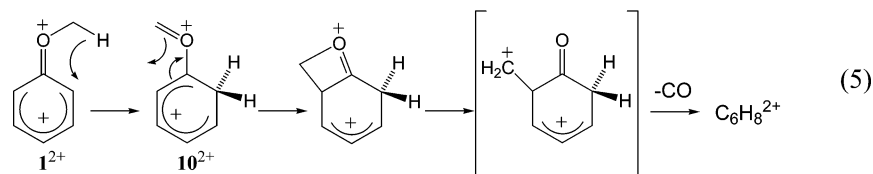
TABLE 3: Mass Spectra of Metastable Dications of *para*-Hydroxyanisole (2), *para*-Dimethoxybenzene (3), *ortho*-Hydroxyanisole (4), *ortho*-Dimethoxybenzene (5), *meta*-Hydroxyanisole (6), and *meta*-Dimethoxybenzene (7)

metastable ion	neutral losses	ion losses
2 ²⁺ ^a	CO (56)	CH ₃ ⁺ (100)
2a ²⁺	CO (4.8)	CD ₃ ⁺ (100)
3 ²⁺	–	CH ₃ ⁺ (100), CD ₃ ⁺ (62)
4 ²⁺ ^a	CO (6.2)	CH ₃ ⁺ (100)
4a ²⁺	CO (2.9)	CD ₃ ⁺ (100)
5 ²⁺	–	CH ₃ ⁺ (100), CD ₃ ⁺ (50)
6 ²⁺ ^a	CO (100)	CH ₃ ⁺ (0.7), HCO ⁺ (0.9), CH ₂ O ⁺ (1.1), C ₂ H ₂ O ⁺ (0.4), C ₂ HO ₂ ⁺ (0.7)
6a ²⁺	CO (100)	¹³ CH ₃ ⁺ (1.0), HCO ⁺ (2.2), ¹³ CH ₂ O ⁺ (1.5), C ₂ H ₂ O ⁺ (0.5), C ₂ HO ₂ ⁺ (0.9)
6b ²⁺	CO (100)	CD ₃ ⁺ (7.6), HCO ⁺ (2.9), CD ₂ O ⁺ (2.9), C ₂ HDO ⁺ (0.7), C ₂ HO ₂ ⁺ (1.8)
6c ²⁺	CO (100)	CH ₃ ⁺ (1.9), HCO ⁺ (1.6), CH ₂ O ⁺ /DCO ⁺ (3.5), C ₂ H ₂ O ⁺ (0.9), C ₂ DO ₂ ⁺ (1.3)
6d ²⁺	CO (100) ^a	CH ₃ ⁺ (1.9), HCO ⁺ (3.9), CH ₂ O ⁺ (3.8), C ₂ H ₂ O ⁺ (1.2), C ₂ HO ¹⁸ O ⁺ (2.5)
7 ²⁺	CO (100), CH ₂ O (12), CHDO (1.4), CD ₂ O (15)	CH ₃ ⁺ (4.6), CH ₃ CO ⁺ (26), CD ₃ CO ⁺ (46), CH ₂ O ⁺ (2.5), CHDO ⁺ (1.4), CD ₂ O ⁺ (2.5), CD ₃ ⁺ (11)

^a The species containing one ¹³C were taken as parent ions, and the intensities are accordingly corrected; see experimental details.

Total electronic energies (E_e), energies at 0 K including ZPVE (E_{0K}) as well as relative energies (E_{rel}) of selected ions are listed in Table 2.

SCHEME 2



Results and Discussion

Anisole. The dominant process in the unimolecular decomposition of the metastable dication formed upon electron ionization of unlabeled anisole corresponds to the loss of a methyl cation concomitant with formation of the monocation $\text{C}_6\text{H}_5\text{O}^+$. In addition, the dication also decomposes via elimination of a neutral CO molecule, which leads to the dicationic fragment $\text{C}_6\text{H}_8^{2+}$. The MI spectra of the labeled compounds $\mathbf{1a}^{2+}$, $\mathbf{1b}^{2+}$, and $\mathbf{1c}^{2+}$ show the same behavior with the expected shifts due to isotopic labeling (Table 1). Charge separation via loss of the methyl substituent is always the main channel and the observed mass differences reflect the labeling pattern without evidence for the occurrence of H/D exchange processes. Thus, the specific losses of $^{13}\text{CH}_3^+$ from $\mathbf{1a}^{2+}$, CD_3^+ from $\mathbf{1b}^{2+}$, and CHD_2^+ from $\mathbf{1c}^{2+}$ indicate a simple heterolytic cleavage of the O–CH₃ bond, leading to the cation $\mathbf{8}^+$ according to reaction 3 (Scheme 2). The calculations predict this process to be exothermic by 0.90 eV (Table 2).

The branching ratio of CO loss is very sensitive to the labeling pattern of the precursor. First, the spectrum of the ^{13}C labeled compound $\mathbf{1a}^{2+}$ shows the loss of CO of mass 28; thus, the expelled CO molecule contains a carbon atom from the arene ring. An initial methyl migration to the ring leading to $\mathbf{9}^{2+}$ (reaction 4 in Scheme 2) does not appear likely, because of the strong apparent kinetic isotope effects (KIEs) observed for the CO loss from the deuterated dications $\mathbf{1b}^{2+}$ and $\mathbf{1c}^{2+}$ (Table 1). In fact, CO loss almost vanishes in the case of $\mathbf{1b}^{2+}$. Accordingly, another mechanism is proposed on the basis of the established fragmentation pathways of the anisole monocation.¹⁰ The rearrangement proceeds stepwise (reaction 5 in Scheme 2): first, a hydrogen atom from the methyl group is transferred to the ring (analogous to reaction 1), which leads to the intermediate $\mathbf{10}^{2+}$, and then a four-membered ring is formed via an electrocyclic process. In contrast to the analogous reaction 1 of the singly charged anisole ion, however, the initial hydrogen migration is not reversible, because otherwise H/D scrambling would occur in the deuterated dications $\mathbf{1b}^{2+}$ and $\mathbf{1c}^{2+}$, respectively, which is not observed experimentally. According to theory, the intermediate $\mathbf{10}^{2+}$ is by 0.62 eV more stable than the anisole dication $\mathbf{1}^{2+}$, which could also explain why the reverse rearrangement does not take place. The second step of reaction 5, the proposed electrocyclic rearrangement of a methylene group, resembles the behavior of the metastable

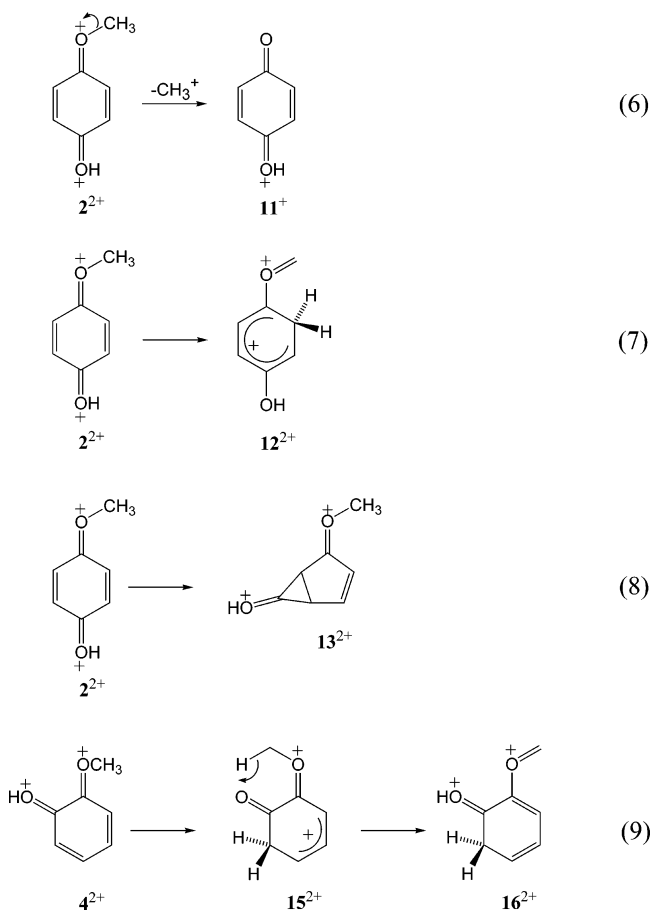
closed-shell phenoxymethylene monocation,¹⁴ where a methylene moiety migrates to the *ortho*-position of the benzene ring via a four-centered transition structure. This scenario of an initial, rate-limiting hydrogen rearrangement in the course of the CO loss can account for the observed diminution of this pathway upon deuteration of the methoxy group.

Obviously, this fragmentation pathway should be assisted by those substituents stabilizing the positive charge in the *meta*-position, whereas the methyl cation elimination (reaction 3) should be assisted by substituents stabilizing a positive charge in the *ortho*- or *para*-position. Accordingly, anisole appears as a suitable probe for the investigation of substituent effects on the dications' chemistry. To this end, OH and OCH₃ groups, respectively, were introduced as additional substituents. The discussion is supported by explorative theoretical studies of the relative stabilities of hydroxy-substituted anisole dications, the respective products of methyl cation elimination and isomeric dications, which are suggested as intermediates in the CO elimination (Table 2). We did not attempt to calculate the whole potential energy surface, since this demanding endeavor is beyond the scope of the present paper; these aspects will be addressed in more detail in a future publication.²³

***Ortho*- and *Para*-Derivatives.** The overall unimolecular fragmentation of *para*-hydroxyanisole dication $\mathbf{2}^{2+}$ is similar to that of the anisole dication, with methyl cation elimination as the major channel. The preference for this process can be attributed to the generation of a stabilized monocation, i.e., protonated *para*-benzoquinone²⁴ $\mathbf{11}^+$ (reaction 6 in Scheme 3), which is also confirmed by a calculated exoergicity of 0.38 eV associated with methyl cation expulsion (Table 2).

Interestingly and perhaps unexpectedly, CO elimination from $\mathbf{2}^{2+}$ is more abundant than in the case of the unsubstituted anisole dication $\mathbf{1}^{2+}$, with a relative intensity of 56% compared to 14% (Tables 1 and 3). A superficial explanation for this difference would evolve from the consideration that the introduction of an OH substituent increases the electron density in the ring and so promotes the first step, i.e., migration of a hydrogen atom from the methyl group to the ring (reaction 7). This effect should be equally operative for the *para*-dimethoxybenzene dication $\mathbf{3}^{2+}$, but no CO loss at all is observed in the MI spectrum of this compound. Moreover, calculations show that the rearrangement of $\mathbf{2}^{2+}$ to $\mathbf{12}^{2+}$ is endothermic by 0.71 eV, which is the consequence of a much better charge

SCHEME 3



stabilization of the parent dication 2^{2+} . An alternative rationale may consider the hidden participation of the hydroxyl group, which can, contrary to a methoxy substituent, undergo keto-enol tautomerism, and thus, a CO molecule can originate from the “phenolic” part of the dication. If this were true, then there should not be a significant kinetic isotope effect upon deuterium labeling of the methoxy substituent ($2a^{2+}$). However, the spectrum of metastable dication $2a^{2+}$ reveals the operation of a profound KIE. The relative diminution of the CO loss in going from 2^{2+} to $2a^{2+}$ is about 90%. It follows that the mechanism, which accommodates all experimental findings, should include involvement of the hydroxyl group as well as the hydrogen migration from the methyl group as key steps on the way to CO elimination. Accordingly, a mechanism is proposed on the basis of an analogy with the rearrangement of the hydroquinone dication:²³ the parent dication 2^{2+} undergoes a quite complex rearrangement to intermediate 13^{2+} (reaction 8); next, a hydrogen atom from the methyl group migrates to the ring and the reaction then proceeds in analogy with reaction 5. Eventually, C–C bond cleavage of the three-membered ring occurs, thus connecting the system to the potential energy surface of the *meta*-derivative 6^{2+} (see below).

As already mentioned above, the dication of *para*-dimethoxybenzene (**3**) does not undergo elimination of CO or any other neutral molecule losses (Figure 1). The mixed labeled derivative 3^{2+} was used, with one methoxy-substituent being labeled with three deuterium atoms. The observed ratio of CH_3^+ versus CD_3^+ elimination is 1.6, indicating a significant secondary kinetic isotope effect²⁵ on the simple cleavage of a C–O bond analogous to reaction 6. The peak shapes—the signals are split into doublets—are a characteristic feature of charge-separation processes;²⁶ thus, a large amount of kinetic energy is released

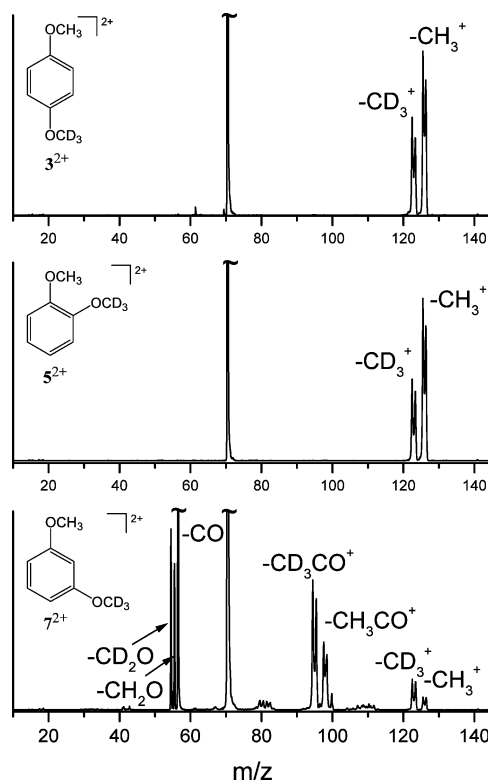


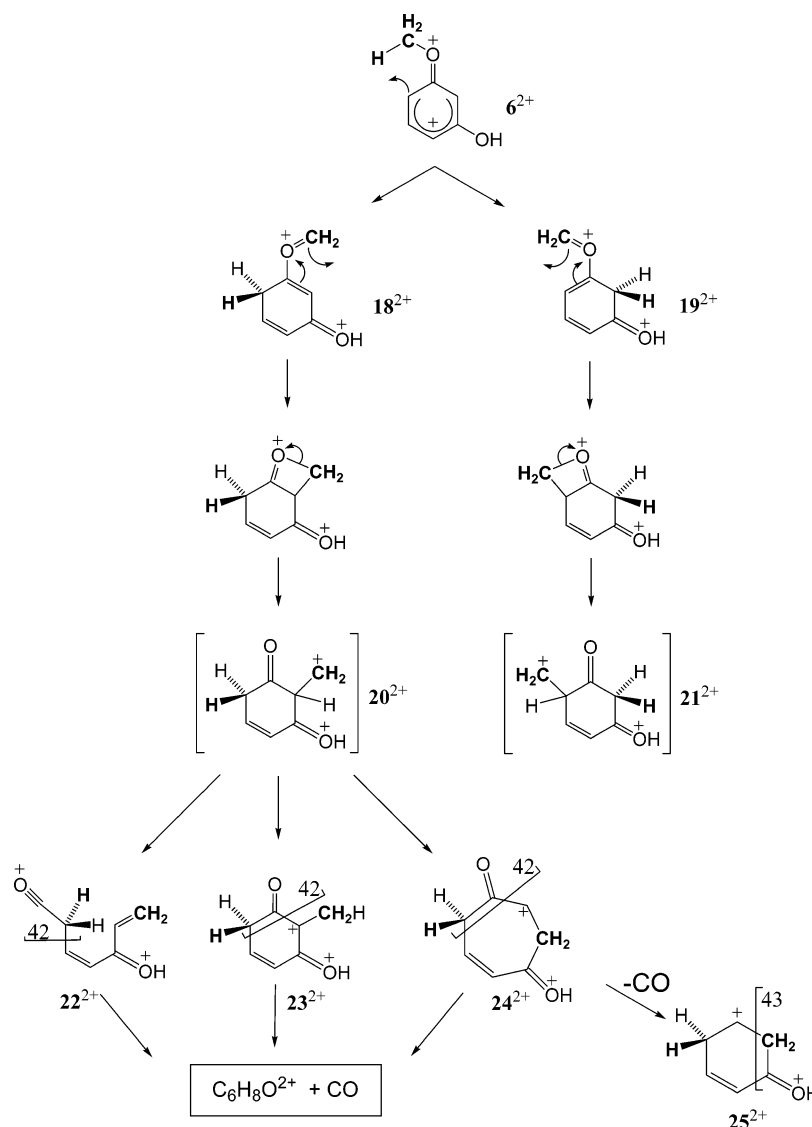
Figure 1. Metastable ion spectra of the dimethoxybenzene dications 3^{2+} , 5^{2+} , and 7^{2+} . The parent ion signals as well as the signal of the fragment ion that corresponds to loss of a CO from 7^{2+} are off-scale. Integrated intensities of peaks are given in Table 3.

once the doubly charged ions break up into two monocations due to Coulomb repulsion.

From the point of view of electronic structures, the fragmentation of *ortho*-derivates should be similar to that of *para*-derivatives, but due to the spatial proximity of the functional groups, also other effects may come into play.⁷ *ortho*-Hydroxy-anisole dication 4^{2+} prevalently decomposes via expulsion of a methyl cation, which leads to the protonated *ortho*-benzoquinone 14^+ . The exoergicity of this process is larger (0.81 eV) than in the case of the *para*-derivative (0.38 eV), which is a consequence of the destabilization of the parent dication 4^{2+} ($E_{rel} = 0.43$ eV) by the vicinity of functional groups and thus charges. The CO-loss channel has considerably lower intensity than in case of the *para*-derivative 2^{2+} , but it is also smaller than for the anisole dication itself. Surprisingly, this trend is reversed for the labeled compound $4a^{2+}$. Dication $4a^{2+}$ gives more CO loss than corresponding labeled anisole dication $1b^{2+}$, and the apparent KIE is much smaller (relative diminution of ca. 50%) than in the case of the *para*-derivatives 2^{2+} and $2a^{2+}$ (ca. 90%). These results suggest the operation of different mechanisms for the hydrogen migration. However, a keto-enol tautomerism, $4^{2+} \rightarrow 15^{2+}$, may be operative in the initial stage, followed by a hydrogen migration from the methyl group to the nearby oxygen, which leads to the intermediate 16^{2+} (reaction 9 in Scheme 3). According to theory, this rearrangement is exoergic by 0.27 eV. The reaction may further proceed via a four-centered transition structure toward the CO-molecule elimination in analogy with reaction 5. Similar to the *para*-derivative **3**, *o*-dimethoxybenzene dication 5^{2+} gives just loss of a methyl cation, and the kinetic isotope effect is comparable for both isomers 3^{2+} and 5^{2+} (Figure 1).

In summary, the metastable dications 2^{2+} , 3^{2+} , 4^{2+} , and 5^{2+} dissociate prevalently via charge separation into two singly charged ions by cleavage of an O–CH₃ bond. The competing

SCHEME 4



CO elimination occurs only after hydrogen rearrangements of 2^{2+} and 4^{2+} , respectively, in which the methyl group plays a decisive role.

Meta-Derivatives. Introduction of a hydroxy-group in the *meta*-position of anisole leads to significant changes in the spectra of the corresponding metastable dications of **6**. The most abundant fragmentation corresponds to the loss of carbon monoxide. This finding is in keeping with the mechanistic picture deduced so far, but yet another factor comes into play: besides the singlet state $^1A'$ of the dication 6^{2+} ($E_{\text{rel}} = 0.87$ eV) also the nearby isoenergetic triplet state $^3A'$ ($E_{\text{rel}} = 0.83$ eV) will be populated and may thus account for the changes in the MI spectra.

In analogy with reaction 5, the introduction of a hydroxy substituent in the *meta*-position increases the electron density in the *ortho*-positions, thus promoting hydrogen rearrangement, and the resulting dications (18^{2+} or 19^{2+}) are then stabilized relative to 6^{2+} (Scheme 4). The calculations show that the singlet state of the dication 18^{2+} (1A) is 0.95 eV more stable than the parent dication 6^{2+} (1A). The dication 19^{2+} (1A) is slightly less energetically favored but nevertheless still 0.75 eV lower in energy than 6^{2+} (1A). On the other hand, the analogous rearrangement of the dication 6^{2+} in the triplet state is endoergic with intermediate 19^{2+} (3A) and 18^{2+} (3A), being 0.76 eV and

1.21 eV higher in energy than the parent dication 6^{2+} ($^3A'$). In conclusion, rather than being involved in the CO-elimination channel, it is expected that the triplet state will contribute to the charge separation leading to the triplet state of protonated *meta*-benzoquinone 17^+ ($^3A''$) and CH_3^+ , a process that is a slightly exoergic reaction ($\Delta E_{\text{rel}} = -0.04$ eV).

CO elimination from 6^{2+} (and its isotopologs) is accompanied by other minor channels, each with intensities less than 3% of the CO loss. To elucidate the mechanism of CO elimination in more detail, the dications of the labeled compounds **6a–d** were examined (Table 3, Figure 2). Upon ^{13}C -labeling of the methyl group (6a^{2+}) as well as ^{18}O -labeling of the hydroxyl group (6d^{2+}), decarbonylation is still associated with a mass difference of $\Delta m = 28$. This result strongly supports the hypothesis that CO elimination proceeds via methylene rearrangement to the ring. The suggested mechanism is analogous to the one proposed for the phenoxymethylene cation¹⁴ and is depicted in Scheme 4. The initial step corresponds to the migration of a hydrogen atom from the methyl group either to the 2- or 6-position of the ring. Next, a series of electrocyclic reactions proceeding via four-membered transition structures leads to the hypothetical intermediates 20^{2+} and 21^{2+} , respectively. As to the CO expulsion, among the many conceivable mechanistic variants that could be proposed, three of them are suggested in Scheme 4

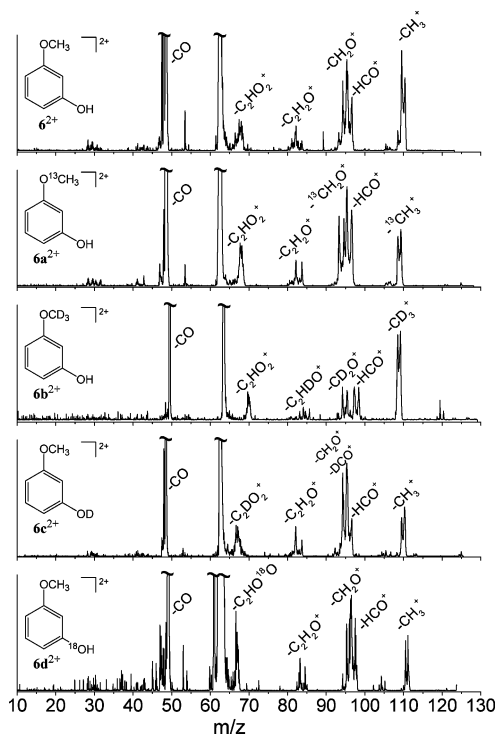


Figure 2. Metastable ion spectra of the dication 6^{2+} and the isotopologs $6a^{2+}$ – $6d^{2+}$. The parent ion signals as well as the signals of fragment ions that correspond to CO loss are off-scale. Integrated intensities of individual peaks or groups of peaks are given in Table 3.

for intermediate 20^{2+} . The first pathway leads to the acyclic species 22^{2+} ; subsequent CO elimination can then be assisted via closure to a five- or six-membered ring. The second route involves a hydrogen transfer from the 2-position of 20^{2+} to the *exo*-methylene group and leads to an intermediate 23^{2+} , followed by CO elimination and the associated contraction to a five-membered ring. The last mechanism suggests an expansion to the seven-membered ring 24^{2+} . Analogous pathways are conceivable for the dissociation of intermediate 21^{2+} .

A closer examination of the spectra of 6^{2+} with respect to the suggested mechanisms starts with an inspection of the methyl cation losses. The relative intensity of this charge-separation process is 1–2%; only for the deuterated dication $6b^{2+}$ does the intensity increase to 8%, which most likely reflects the operation of a conventional KIE. Interestingly, the intensity of the CD_3^+ signal increases not only relative to the CO loss but also in comparison to all other signals present in the spectrum. This suggests that all other fragmentations commence with a hydrogen migration from the methyl group to the ring and are therefore subject to the operation of a primary kinetic isotope effect when comparing 6^{2+} and $6b^{2+}$. Further characterization of these fragments will thus shed light on the overall mechanism. The next monocationic fragment corresponds to the loss of a cation with $m/z = 29$. This mass difference persists for all of the labeled compounds investigated and is therefore assigned to a HCO^+ fragment;²⁷ formation of $C_2H_5^+$ is highly improbable, because as evidenced by the spectra of dication $6b^{2+}$ this would require inclusion of all hydrogen atoms from the ring plus a hydrogen from the hydroxy group. HCO^+ elimination from the phenolic part of the dication can be excluded as well, because it would have to be reflected in the MI spectra of $6c^{2+}$ and $6d^{2+}$ by corresponding mass shifts. Further, the HCO^+ fragment also does not originate from the methoxy group alone, because this would lead to the elimination of $H^{13}CO^+$ from $6a^{2+}$. Accordingly, again a hydrogen rearrangement commencing at

the methoxy group is proposed to precede the dissociation. A possible explanation evolves once more from consideration of Scheme 4. Prior to the dissociation of intermediates 20^{2+} and 21^{2+} , respectively, one of the H atoms originally attached to the ring migrates to the CO group. If the hydrogen rearrangement from the ring to the CO group would proceed statistically, the loss of DCO^+ from $6b^{2+}$ should be observed. Since the corresponding signal is not detected (Figure 2), the hydrogen rearrangement proceeds most probably specifically or is associated with a strong KIE. In this context, it is also worth noting that the ratio of HCO^+ to CH_2O^+ elimination from 6^{2+} is roughly 1:1 and it remains unchanged upon labeling for $6a^{2+}$, $6b^{2+}$, and $6d^{2+}$. Only in the case of $6c^{2+}$, which bears a deuterium labeled phenolic group, the amount of HCO^+ is somewhat lowered, whereas the signal corresponding to the isobaric losses of CH_2O^+ and DCO^+ is relatively higher. Similar to *meta*-dihydroxybenzene cation,²⁸ the keto–enol tautomerism between the phenolic group and adjacent carbon atoms of the ring can be expected for the dication 6^{2+} , which can also account for the scrambling of hydrogens between the ring and the phenolic group. Finally, the departing CO molecule can be protonated by a proton transfer from the phenolic group, or the proton is transferred from the carbon of the ring as proposed above. In any case, the presence of the loss of DCO^+ from the $6c^{2+}$ dication on one hand and its absence from the $6b^{2+}$ dication on the other hand suggest the operation of a specific mechanism in the elimination of the HCO^+ ion.

A minor route of charge separation leads to the formation of a $C_2H_2O^+$ cation from 6^{2+} . Inspection of the labeling data (Figure 2) is quite revealing, and the reaction mechanism shown in Scheme 4 suggests formation of the $C_2H_2O^+$ fragment via the decomposition depicted with the label “42” in the hypothetical dications 22^{2+} , 23^{2+} , and 24^{2+} . This scenario is in keeping with the observed shifts of the fragment masses in the case of the dication $6b^{2+}$, because one of the hydrogen atoms is replaced by a deuterium (depicted by bold H), and the exclusive formation of $C_2H_2O^+$ from all remaining isotopologs of 6^{2+} . Finally, the mass differences of $\Delta m = 57$ (6^{2+} , $6a^{2+}$, $6b^{2+}$), 58 ($6c^{2+}$), and 59 ($6d^{2+}$) are assigned to sequential eliminations of CO and HCO^+ (DCO^+ and $HC^{18}O^+$, respectively, for $6c^{2+}$ and $6d^{2+}$). The expulsion of both oxygen atoms (as CO and HCO^+) in the course of the dication fragmentation is consistent with a cyclic structure of the dication intermediate after losing CO (e.g. 25^{2+} in Scheme 4).

As a further step toward understanding the mechanism of decarbonylation of 6^{2+} , the collisional activation spectra of the fragment ions after unimolecular loss of CO are considered (MI/CA spectra, Figure 3). While the base peak corresponds to a charge-exchange process of the parent dication with the collision gas O_2 , among other peaks, several characteristic features can be found. In the MI/CA spectrum of $[6^{2+} - CO]$, a signal at $m/z = 43$ can be identified. This ion mass suggests the composition CH_3CO^+ ,²⁹ because $C_3H_7^+$ appears unlikely. Upon ^{13}C -labeling, in the MI/CA spectrum of $[6a^{2+} - CO]$, the signal undergoes a shift to $m/z = 44$, hence $^{13}CH_3CO^+$. For the deuterated dication $[6b^{2+} - CO]$, the formation of $m/z = 45$, i.e., CHD_2CO^+ , is observed (although also some minor H/D scrambling can be identified in this spectrum). These results suggest that the fragment ion with $m/z = 43$ has incorporated the carbon atom of the methoxy substituent in 6^{2+} , which has to be adjacent to the phenolic group upon loss of CO molecule. All experimental findings are in favor of the reaction pathway $6^{2+} \rightarrow 18^{2+} \rightarrow 20^{2+} \rightarrow 24^{2+} \rightarrow 25^{2+}$. The loss of the appropriate fragment is depicted with the label “43” in structure 25^{2+} .

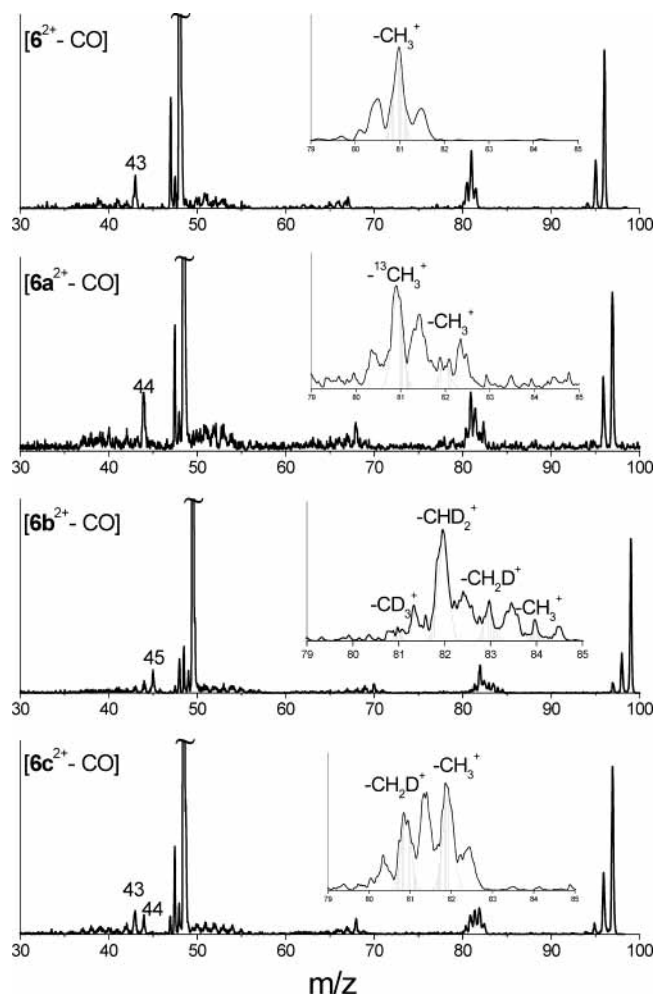


Figure 3. Collisional activation spectra (collision gas O_2) of fragment ions originating from the unimolecular dissociations of dication 6^{2+} and some isotopologs via loss of a CO molecule. The parent ion signals are off-scale.

Interestingly, the dication $[6^{2+} - CO]$ also undergoes the elimination of neutral H_2 . The driving force of this process is presumably the formation of an energetically favorable dication, e.g., elimination of molecular hydrogen from 25^{2+} may yield—after some rearrangements—the dication of phenol.

Let us now address the insets in Figure 3, which display the multiplets of peaks that correspond to losses of either a methyl cation from the dication or a methyl radical from the molecular monocations after charge exchange has taken place. The unlabeled dication $[6^{2+} - CO]$ loses mass 15. The origin of the fragment ions is reflected in the composite shape of the peak, which is sketched in Figure 4. The central peak corresponds to a process with a relatively small kinetic energy release and is thus assigned to the decomposition of singly charged ion. In contrast, the “doublet” corresponds to a process with a high kinetic-energy release (depicted by a horizontal arrow) and thus reflects the Coulomb explosion of the dication. The central components are shaded in the insets of Figure 3 for an easier orientation. Interestingly, the selectivities are different for the direct loss of a methyl cation from the dication and the sequence of events in which charge-exchange is followed by fragmentation of the monocation. The MI/CA spectrum of the ^{13}C labeled fragment ion $[6a^{2+} - CO]$ shows that upon charge exchange with O_2 the monocation $[6a^{+} - CO]$ loses preferentially a methyl radical with incorporation of the ^{13}C -atom. Similarly, the deuterated monocation $[6b^{+} - CO]$, which is formed by charge

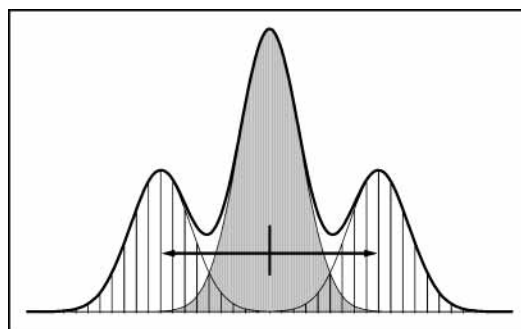


Figure 4. Sketch of a composite peak, which can be found in the collisional activation spectra of dications. The central part (shaded area) corresponds to the dissociation of the singly charged parent ion formed by charge exchange between the dication and the collision gas, whereas the “doublet” (hatched area) reflects the genuine Coulomb explosion of the dication.

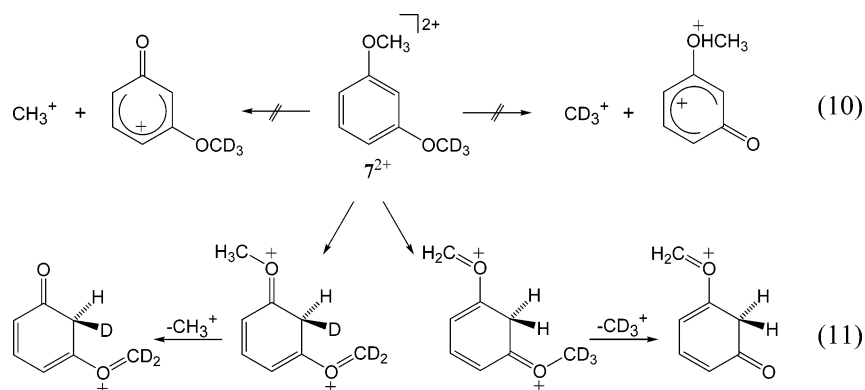
exchange from $[6b^{2+} - CO]$ loses preferentially CHD_2^+ , which corresponds to the same fragment (bold structure in Scheme 4). On the other hand, the direct methyl cation loss from the corresponding dications is less specific, as can be observed in the spectrum of $[6b^{2+} - CO]$. Accordingly, extensive hydrogen rearrangements precede Coulomb explosion.

The spectrum of metastable *meta*-dimethoxybenzene (7^{2+}) lends further support to the suggested fragmentation scheme. The base peak in the MI spectrum of this mixed-labeled compound is, as expected, due to the elimination of CO (Figure 1). The CH_3^+ loss has a relative intensity of 5% compared to 11% for CD_3^+ ; the ratio CH_3^+/CD_3^+ is ~ 0.4 . The inverse kinetic isotope effect suggests that the mechanism of methyl cation elimination starts with a “hidden” hydrogen rearrangement,^{30,31} rather than being a simple cleavage (reaction 10 in Scheme 5) of a $O-CH_3$ bond as appears to be the case for the *ortho*- and *para*-derivatives. The difference is fundamental and probably associated again with the electronic structure of the dication. Thus, the methoxy substituent in the *meta*-position, similar to a hydroxy substituent, facilitates hydrogen migration to the ring to afford the isomeric dications, which are expected to be relatively more stable with respect to the parent dication 7^{2+} (analogous to the rearrangement $6^{2+} \rightarrow 18^{2+}$ or 19^{2+}). The isomeric dications can eventually undergo charge separation (reaction 11 in Scheme 5).

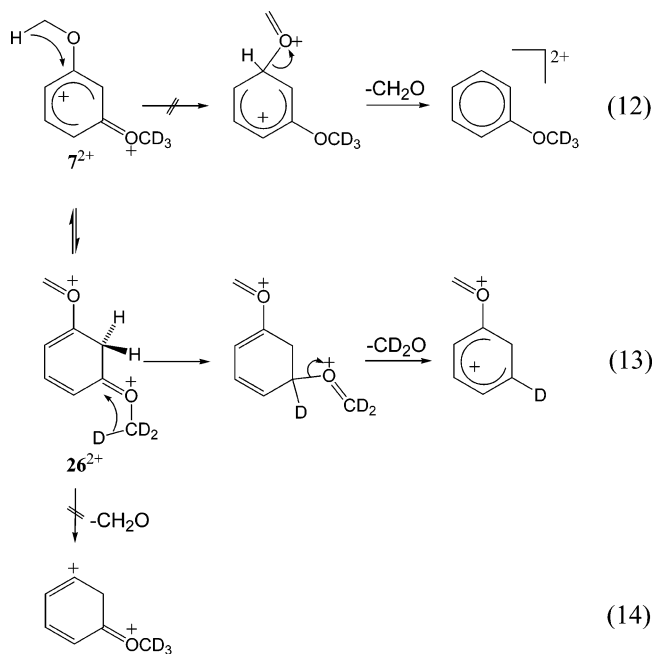
Similar inverse kinetic isotope effects are operative in all other monocation losses from the dication 7^{2+} . The most abundant cation losses correspond to $m/z = 43$ (intensity 26%) and $m/z = 46$ (intensity 46%), respectively. They most probably originate from sequential elimination of CO and a methyl cation rather than an intact CH_3CO^+ cation,²⁹ because the latter is expected to be observed experimentally, which is not the case.

Besides CO elimination, dication 7^{2+} also loses the neutral formaldehyde molecules CH_2O and CD_2O , respectively, in a 1:1.3 ratio. The apparent KIE indicates that the mechanism of formaldehyde elimination from one of the methoxy substituents is preceded by a hydrogen migration from the other methoxy substituent. This requirement disfavors the mechanism depicted in reaction 12 (Scheme 6). An alternative mechanism involves an initial hydrogen migration $7^{2+} \rightarrow 26^{2+}$. Further, the dication 26^{2+} is suggested to not directly eliminate CH_2O (reaction 14 in Scheme 6), as this mechanism would not result in the observed inverse KIE. Instead, by analogy to reaction 1, we suggest that the hydrogen from the second methoxy group migrates to the ring, which is followed by CD_2O elimination (reaction 13 in Scheme 6). The apparent KIE for the $CH_2O/$

SCHEME 5



SCHEME 6



CD_2O losses is smaller than in the case of the charge-separation process, and several scenarios can contribute to this finding. First, reactions 12 and 14 can also take part to some extent, which would act in an opposite direction as far as KIEs are concerned.²⁵ The second reasoning is related to reaction 13 itself. If the initial hydrogen migration is followed by the migration of hydrogen from the second methoxy group, due to the labeling pattern of **7**, one inevitably encounters migration of both H and D prior to fragmentation. Consequently, the overall apparent KIE probed experimentally is then the sum of two opposing individual KIEs.

In summary, the introduction of OH or OCH_3 substituents to the *meta*-position of anisole dication drastically alters the reactivity in that hydrogen migration to the ring is strongly preferred and precedes all subsequent processes. Accordingly, an answer to the question raised at the beginning of this study can be provided: the fragmentation of metastable anisole dication is not necessarily entirely controlled by direct charge-separation processes but instead proceeds via bound dication states until an appropriate structure is reached from which charge separation can occur. As a consequence, the dication fragmentation is strongly influenced by the substitution pattern, as demonstrated by a comparison of the spectra shown in Figure 1: The KIE for methyl cation elimination from *ortho*- and *para*-dimethoxybenzene dication is roughly $\text{CH}_3^+:\text{CD}_3^+ \sim 2:1$,

TABLE 4: Mass Spectra of Metastable Dications Derived from *para*-, *ortho*-, and *meta*-Anisidine (27**, **28**, and **29**, respectively)**

metastable ion	neutral losses	ion losses
27 ²⁺	CO (27)	CH_3^+ (100)
28 ²⁺	CO (24)	CH_3^+ (100)
29 ²⁺	CO (100), CH_2O (0.8)	HCO^+ (0.7), CH_2O^+ (0.8), CH_3O^+ (2.0), CH_3^+ (<0.5)

whereas the *meta*-dimethoxybenzene dication eliminates a methyl cation in a ratio $\text{CH}_3^+:\text{CD}_3^+ \sim 1:2$.

To probe the proposed operation of a strong substituent effect on the unimolecular dissociation of the anisole dication, the corresponding amino-substituted dications derived from *ortho*-, *meta*-, and *para*-anisidines (aminoanisoles) were briefly examined as well. The spectra of metastable *para*- and *ortho*-anisidine dications **27**²⁺ and **28**²⁺, respectively, bear methyl cation losses as major channels, whereas the elimination of CO prevails for the *meta*-derivative **29**²⁺ (Table 4). In fact, only a very small signal due to the loss of a methyl cation is observed in the spectrum of the *meta*-anisidine dication, which suggests that the amino group has a stronger substituent effect than the hydroxy group. The MI/CA spectrum of the dication [**29**²⁺ – CO] formed by CO elimination from metastable *meta*-anisidine dication **29**²⁺ shows somehow a similar pattern as the dication [**6**²⁺ – CO], but the most abundant process is the elimination of molecular hydrogen.

Conclusions

The fragmentations of substituted anisole dications follow two principal directions. Either elimination of a methyl cation occurs via cleavage of the O– CH_3 bond or dissociation begins with the migration of a hydrogen atom from the methyl group to the ring, which promotes subsequent processes (CO elimination or charge-separation reactions). The nature of the fragmentation is quite sensitive to substitutions with OH, OCH_3 , and NH_2 groups, respectively. Upon substitution of the anisole dication at the *ortho*- or *para*-position, the formation of a methyl cation is favored. Introduction of the substituent in the *meta*-position completely switches the reactivity in favor of hydrogen rearrangement. The dominant channel is then CO elimination. Methyl cation is only formed after hydrogen migration to the phenyl ring, as revealed by the operation of inverse H/D kinetic isotope effects. Accordingly, several general conclusions evolve from this study:

(1) Observation of regioselective reactions proves that—at least in part—the connectivities of the neutral precursors remain intact in the dication states.

(2) H/D-labeling reveals that there is even less equilibration ("scrambling") in the dissociation of the metastable dications than in the fragmentation of the corresponding monocations.

(3) The dication behavior is not necessarily driven by Coulomb repulsion only but can proceed with several bond-forming steps and bond cleavages until a preferable structure for charge separation is reached.

Acknowledgment. Continuous financial support by the European Commission (MCInet), the Deutsche Forschungsgemeinschaft, the Fonds der Chemischen Industrie, and the Gesellschaft von Freunden der Technischen Universität Berlin is gratefully acknowledged.

References and Notes

- (1) Mathur, D. *Phys. Rep.* **1993**, 225, 193.
- (2) Schröder, D.; Schwarz, H. *J. Phys. Chem. A* **1999**, 103, 7385.
- (3) Vekény, K. *Mass Spectrom. Rev.* **1995**, 14, 195.
- (4) Gill, P. M. W.; Radom, L. *J. Am. Chem. Soc.* **1988**, 110, 5311.
- (5) Nenajdenko, V. G.; Shevchenko, N. E.; Balenkova, E. S. *Chem. Rev.* **2003**, 103, 229.
- (6) Kingston, D. G. I.; Hobrock, B. W.; Bursley, M. M.; Bursley, J. T. *Chem. Rev.* **1975**, 75, 693.
- (7) Schwarz, H. *Top. Curr. Chem.* **1978**, 73, 231.
- (8) Kuck, D. *Mass Spectrom. Rev.* **1990**, 9, 583.
- (9) Kuck, D. *Int. J. Mass Spectrom.* **2002**, 213, 101.
- (10) Cooks, R. G.; Bertrand, M.; Beynon, J. H.; Rennekamp, M. E.; Setser, D. W. *J. Am. Chem. Soc.* **1973**, 95, 1732.
- (11) Aviyente, V.; Elam, M.; Ohmichi, N.; Lifshitz, C. *J. Phys. Chem.* **1988**, 92, 6548.
- (12) Das, P. R.; Gilman, J. P.; Meisels, G. G. *Int. J. Mass Spectrom. Ion Processes* **1986**, 68, 155.
- (13) Ziesel, J. P.; Lifshitz, C. *Chem. Phys.* **1987**, 117, 227.
- (14) Molenaar-Langeveld, T. A.; Ingemann, S.; Nibbering, N. M. M. *Org. Mass Spectrom.* **1993**, 23, 1167.
- (15) Srinivas, R.; Sülzle, D.; Weiske, T.; Schwarz, H. *Int. J. Mass Spectrom. Ion Processes* **1991**, 107, 368.
- (16) Vosko, S. H.; Wilk, L.; Nusair, M. *Can. J. Phys.* **1980**, 58, 1200.
- (17) Lee, C.; Yang, W.; Parr, R. G. *Phys. Rev. B* **1988**, 37, 785.
- (18) Miehl, B.; Savin, A.; Stoll, H.; Preuss, H. *Chem. Phys. Lett.* **1989**, 157, 200.
- (19) Dunning, T. H., Jr. *J. Chem. Phys.* **1989**, 90, 1007.
- (20) Kendall, R. A.; Dunning, T. H., Jr.; Harrison, R. J. *J. Chem. Phys.* **1992**, 96, 6796.
- (21) Woon, D. E.; Dunning, T. H., Jr. *J. Chem. Phys.* **1993**, 98, 1358.
- (22) Frisch, M. J.; Trucks, G. W.; Schlegel, H. B.; Scuseria, G. E.; Robb, M. A.; Cheeseman, J. R.; Zakrzewski, V. G.; Montgomery, J. A., Jr.; Stratmann, R. E.; Burant, J. C.; Dapprich, S.; Millam, J. M.; Daniels, A. D.; Kudin, K. N.; Strain, M. C.; Farkas, O.; Tomasi, J.; Barone, V.; Cossi, M.; Cammi, R.; Mennucci, B.; Pomelli, C.; Adamo, C.; Clifford, S.; Ochterski, J.; Petersson, G. A.; Ayala, P. Y.; Cui, Q.; Morokuma, K.; Malick, D. K.; Rabuck, A. D.; Raghavachari, K.; Foresman, J. B.; Cioslowski, J.; Ortiz, J. V.; Baboul, A. G.; Stefanov, B. B.; Liu, G.; Liashenko, A.; Piskorz, P.; Komaromi, I.; Gomperts, R.; Martin, R. L.; Fox, D. J.; Keith, T.; Al-Laham, M. A.; Peng, C. Y.; Nanayakkara, A.; Gonzalez, C.; Challacombe, M.; Gill, P. M. W.; Johnson, B. G.; Chen, W.; Wong, M. W.; Andres, J. L.; Head-Gordon, M.; Replogle, E. S.; Pople, J. A. *Gaussian 98*, revision A.11; Gaussian, Inc.: Pittsburgh, PA, 1998.
- (23) Roithová, J.; Schröder, D.; Schwarz, H. To be submitted.
- (24) Irikura, K. K.; Meot-Ner, M.; Sieck, L. W.; Fant, A. D.; Liebman, J. F. *J. Org. Chem.* **1996**, 61, 3167.
- (25) Frosig, L.; Hammerum, S. *Adv. Mass Spectrom.* **1998**, 14, A017250/1.
- (26) Cooks, R. G.; Beynon, J. H.; Caprioli, R. M.; Lester, G. R. *Metastable Ions*; Elsevier: Amsterdam, 1973.
- (27) Although $m/z = 29$ may correspond to HCO^+ as well as to COH^+ structures, we assign the fragment to the first one that is strongly preferred energetically; see: Bouma, W. J.; Burgers, P. C.; Holmes, J. L.; Radom, L. *J. Am. Chem. Soc.* **1986**, 108, 1767.
- (28) Gerhards, M.; Unterberg, C.; Schumm, S. *J. Chem. Phys.* **1999**, 111, 7966.
- (29) The $\text{C}_2\text{H}_3\text{O}^+$ ion may correspond to isomeric structures CH_3CO^+ and CH_2COH^+ , respectively, of which the former is more stable; see: (a) Drewello, T.; Schwarz, H. *Int. J. Mass Spectrom. Ion Processes* **1989**, 87, 135. (b) Koch, W.; Schwarz, H.; Maquin, F.; Stahl, D. *Int. J. Mass Spectrom. Ion Processes* **1985**, 67, 171. (c) Vogt, J.; Williamson, A. D.; Beauchamp, J. L. *J. Am. Chem. Soc.* **1978**, 100, 3478.
- (30) Schwarz, H. *Top. Curr. Chem.* **1981**, 97, 1.
- (31) Ahlberg, P.; Thibblin, A. *J. Chem. Soc. Rev.* **1989**, 18, 209.